Table 2. The non-conserved residues of HLA-DPs that affect the properties of the peptide-binding grooves

| HLA–DP | Peptide–binding groove | | | | | |
|---|---|---|---|---|---|---|
| | Position 31(α) | Position 84(β) | Position 69(β) | Position 11(α) | Position 35(β) | Position 55(β) |
| HLA–DP5[a] | Q (P1) (charge) | D (P1) (charge) | K (P4) (closed) | M (P6) (depth) | L (P9) (depth) | E (P9) (width) |
| HLA–DP2[b] | M (P1) | G (P1) | E (P4) (open) | A (P6) | F (P9) | D (P9) |

[a] *DPA1*02:02* and *DPB1*05:01*.
[b] *DPA1*01:03* and *DPB1*02:01*.
Blue boxes: The position involves divergent residues based on *DPA1* and *DPB1* four-digit allele-level typing.
Green boxes: The position involves divergent residues identified by comparing the structures of HLA-DP5 • Cry j 1 and HLA-DP2 • pDRA.

determined by positions p4 and 13(β) in the β1 domain (Fig. 3i). The distances in the HLA-DP5 and HLA-DP2 structures are 8.40 Å (the longest) and 8.06 Å, respectively, while the average value in the other class II major histocompatibility complex/HLA structures is 6.54 Å [25]. A superimposition of HLA-DP5 bound with the Cry j 1 peptide onto HLA-DP2 bound with pDRA (Fig. 3c) revealed that the position of Phe(p6) of Cry j 1 is shifted up by the side chain of Met11α, as compared with Phe(p6) of pDRA. The main chain of Ala(p5) of Cry j 1 is consequently pushed up (Fig. 3d), which facilitates its characteristic interaction with Lys69α(HLA-DP5) (Fig. 3f). The amino acid sequence of HLA-DP5 is highly homologous to that of HLA-DP2, with a sequence identity of 95%. Six of the seventeen non-conserved residues are clustered in the peptide-binding groove: Met11 and Gln31 of the α chain; Leu35, Glu55, Lys69, and Asp84 of the β chain of HLA-DP5 (Fig. 3j). It should be emphasized here that these non-conserved residues participate in the formation of the P1, P4, P6, and P9 pockets, as described above, to achieve the distinct specificities of the peptide binding by HLA between HLA-DP5 and HLA-DP2.

### Evolutionary analysis of HLA-DP alleles in the peptide-binding region

To scrutinize the non-conserved residues between HLA-DP5 and HLA-DP2, we constructed phylogenetic trees based on the synonymous substitutions under the molecular clock hypothesis (Fig. 4a and b; Supplementary Fig. 1a). In both the *DPA1* and *DPB1* trees, the extent of synonymous divergence was about 4% between HLA-DP2 and HLA-DP5, which represents divergence 20 million years ago, using a synonymous substitution rate of $10^{-9}$/site/year. Thus, HLA-DP2 and HLA-DP5 diverged long ago. Since then, the *DPA1* and *DPB1* genes have accumulated further lineage-specific amino acid substitutions, and each formed the DP2 and DP5 groups with multiple members (Fig. 4a and b; Supplementary Fig. 1b and c). Especially, the amino acid substitutions involving Met11α and Gln31α in the peptide-binding region (PBR) of the DP5 group occurred twice in the newly created branches ("the external branches"), and moreover, those involving Asp84β of the DP5 group occurred in the differentiation of the DP2 and DP5 groups (Fig. 4a and b; Supplementary Fig. 1b–e). Three residues, Met11α, Gln31α, and Asp84β, are "non-conserved" between HLA-DP5 and HLA-DP2 (Fig. 3j) and are also relevant to the distinct peptide-binding specificities. Notably, Gln31α and Asp84β form the negatively charged P1 pocket in HLA-DP5. Thus, the crystal structure, together with structural comparisons and evolutionary analyses, revealed the specific differentiation of the P1 pocket in the HLA-DP family.

## Discussion

In our previous study, we observed a statistically significant association between HLA-DP5 and susceptibility to Japanese cedar pollinosis. We also identified a dominant epitope, Cry j 1(208–227), which was recognized in the context of HLA-DP5 by $CD4^+$ Th2 cells in many patients with Japanese cedar pollinosis [22,23]. Therefore, we thought that the HLA-DP5-associated susceptibility to Japanese cedar pollinosis may be explained by HLA-DP5-mediated antigen presentation of the major Cry j 1 epitope to Th2 cells producing interleukin-4, an essential cytokine for IgE production by antibody-secreting plasma cells. Subsequently, the core 9-mer Cry j 1(214-KVTVAFNQF-222) peptide presented by HLA-DP5 was identified [22].

In the present study, we determined the crystal structure of HLA-DP5 bound with this 9-mer Cry j 1 core peptide. In the structure, the peptide-binding groove formed by the HLA-DP5α and HLA-DP5β chains recognizes the KVTVAFNQF sequence (Fig. 1), which corresponds exactly to the minimal peptide previously proposed by *in vitro* experiments [22]. Furthermore, we confirmed that HLA-DP5 exhibits the same Cry j 1-binding mode in solution,

through pull-down experiments using structure-based mutations of Cry j 1(9-mer) (Fig. 2).

Previous four-digit allele-level typing studies of the *DPA1* and *DPB1* alleles indicated that the residues at positions 31(α), 56(β), and 85–87(β) are "non-conserved" in the DP alleles (Table 2) [27]. In addition, we compared the structures of the HLA-DP5•Cry j 1 and HLA-DP2•pDRA complexes and identified the characteristic positions that are responsible for the distinct properties between HLA-DP5 and HLA-DP2, with regard to the peptide-binding mode (Table 2). In the present peptide-binding mode, the Lys residue at the Cry j 1(p1) position is a specific anchor residue, as it forms a salt bridge with the negatively charged P1 pocket of HLA-DP5. The bottom of the p1 pocket consists of the "non-conserved" residues at positions 31(α) and 84(β) and may accommodate different kinds of side chains between HLA-DP5 and HLA-DP2 (Fig. 3a, b, and e). Similarly, Leu and Glu at positions 35(β) and 55(β), respectively, of HLA-DP5 alter the shape of the p9 pocket, as compared to that of the P9 pocket involving Phe35(β) and Asp55(β) of HLA-DP2 (Fig. 3a, b, and h). Overall, the "non-conserved" residues on the peptide-binding groove of HLA-DP5 generate its distinct pocket properties from those of HLA-DP2. Therefore, the HLA-DP5•Cry j 1 complex forms 10 hydrogen bonds between the groove and the peptide (Fig. 2a), while these features are not observed in the HLA-DP2•pDRA complex [25] (Fig. 2b).

Moreover, the Cry j 1(p5) position is pushed up by Lys at position 69(β), in collaboration with Met at position 11(α) of HLA-DP5, in the HLA-DP5•Cry j 1 complex (Fig. 3c, d, and f; Table 2). The region around the p4 and p5 positions of the peptide is frequently recognized by complementarity determining region 3 of the specific T cell receptor [28], and the conformational features at the p5 position may allow the peptide to escape from negative selection in the thymus. In the HLA-DP2•pDRA crystal, the complex adopted the auto-inhibited conformation for beryllium (Be), by association with the N-terminal Arg(p−2) of pDRA and the neighboring acidic pocket of HLA-DP2 [25]. However, in the present HLA-DP5 structure, none of the peptide residues are inserted in the pocket because the Lys at position 69(β) of HLA-DP5 occupies the space (Fig. 3f and Table 2). This is also relevant to the proposal by Dai *et al.* [25], who noted that a Lys residue at the p4 position of an HLA-DP2-binding peptide may not allow Be binding.

The evolutionary analysis revealed that the Met11α, Gln31α, and Asp84β residues, which are characteristic of HLA-DP5, are responsible for its distinct peptide binding features. First, Gln31α and Asp84β are critical for the specificity of the P1 pocket

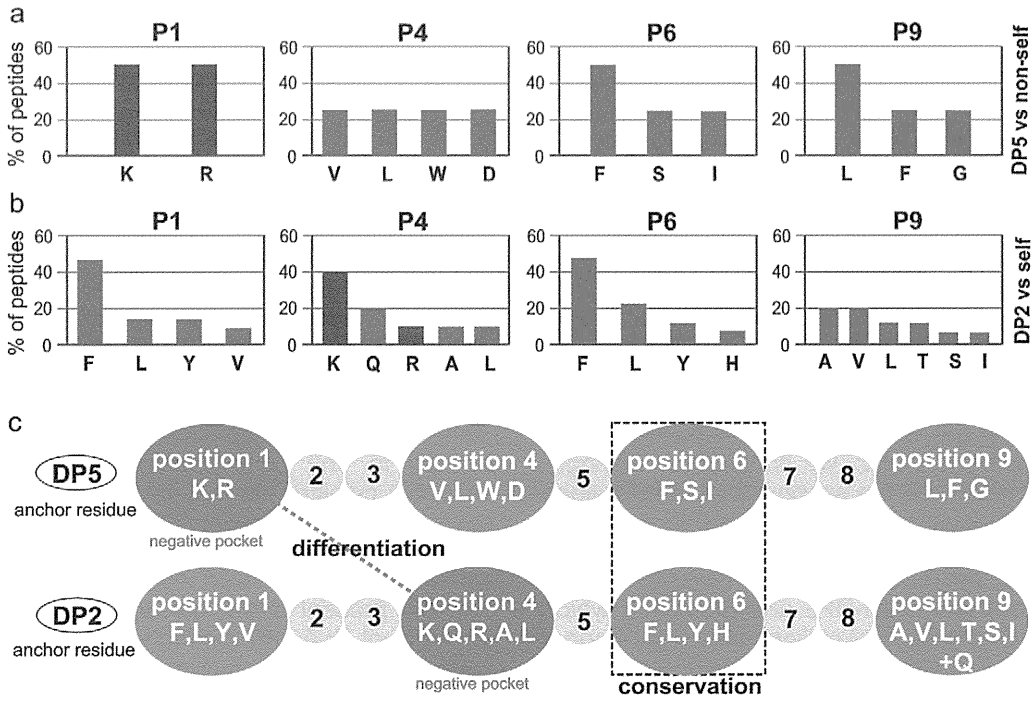


**Fig. 5.** Comparison of the peptide-binding motifs and the pocket properties between HLA-DP5 and HLA-DP2. Amino acid residues of the main anchor positions frequently detected in the non-self-peptides bound to HLA-DP5 (a) and the self peptides bound to HLA-DP2 (b). (a and b) Calculations included only the longer peptide sequences from each source protein. (b) The chart constructed by using examples from a previous report [29]. (c) Relationships between the peptide-binding motifs and the pocket properties of HLA-DP5 and HLA-DP2.

for the positively charged Lys(p1) residue (Fig. 3e). Second, Met11α is involved in the mechanism underlying the pushed-up position of the Phe(p6) residue (Fig. 3d). This finding suggested that the substitutions in the PBR could have been responsible for the diversification of the peptide-binding mode within the DP5 group. Interestingly, Met11α of HLA-DP5 and Ala11α of HLA-DP2 are coupled with Lys69β and Glu69β, respectively (Table 2), to form the haplotype-specific peptide-binding modes described above. Furthermore, Leu35β of HLA-DP5 and Phe35β of HLA-DP2 are coupled with Glu55β and Asp55β, respectively (Table 2), and these interactions are important for the formation of the different pocket sizes between HLA-DP5 and HLA-DP2. These replacements occurred when the two groups branched apart 20 million years ago.

Three other epitope peptides of Cry j 1/2 [Cry j 1 (61–75), Cry j 2 (81–95), and Cry j 2 (336–350)] reportedly interact with HLA-DP5 [23]. Considering that the negatively charged P1 pocket with Gln31α is the major characteristic of the DP5 group, we assigned a positively charged residue, K or R, in the epitope peptides to the p1 position and then examined if residues p2–p9 are compatible with the properties of the corresponding pockets of HLA-DP5 (Supplementary Table 1a). Furthermore, we preliminarily modeled the epitope peptides within the peptide-binding groove, on the basis of the present HLA-DP5•peptide complex structure (Supplementary Fig. 2a–c). Thus, we found that these peptides fit well not only in the P1 pocket but also in the P6 and P9 pockets and form 9–10 hydrogen bonds in total, indicating that the assignment of K/R to p1 is reasonable (Fig. 5a and Supplementary Table 1a). Consequently, we concluded that the peptide-binding groove of the DP5 group can bind the epitope peptides bearing p1Lys/Arg, with a certain allowance for the other pockets.

On the other hand, 27 peptides, including Cry j 2 (185–193), reportedly associate with HLA-DP2 [23,29,30]. Considering the HLA-DP2•pDRA complex structure, we assigned the aromatic residues, F or Y, in these epitope peptides to the p1 and p6 positions and examined if their residues p2–p5/p7–p9 are compatible with the peptide-binding groove of HLA-DP2 (Supplementary Table 1b). Moreover, we constructed several preliminary structural models (Supplementary Fig. 2d and e). The p1 and p6 side chains fit well in their corresponding pockets, and 4–5 hydrogen bonds are formed in total. Interestingly, Lys(p4) is most frequently observed for the DP2 epitope peptides (Fig. 5b and Supplementary Table 1b) and fits nicely within the negatively charged P4 pocket of HLA-DP2. Actually, the epitope peptide with the putative optimal residues, Phe(p1), Lys(p4), and Phe(p6), has been found [29], whereas the other peptides have suboptimal side chains at either p1/p6 or p4. In the case of the HLA-DP2•pDRA complex structure, the lack of Lys(p4) in pDRA, which has Leu(p4) instead, is compensated by the bound Be ion. It was previously argued that the pDRA/Be-binding mode of HLA-DP2 is probably different from the others [25,31]. Overall, the peptide-binding groove of the DP2 group can bind these epitope peptides with a certain allowance.

For both the DP5 and DP2 groups, the properties of the P6 pocket have been conserved to accommodate an aromatic side chain in the course of evolution (Fig. 5c). In contrast, the DP5 and DP2 groups differentially acquired the negatively charged pocket at the P1 and P4 positions, respectively (Fig. 5c). It is likely that this evolutionary diversification of the peptide-binding groove created the specificities of the HLA-DP family members to cover the present diversity of the epitope peptides.

The present crystal structure, together with the structural comparisons and evolutionary analyses, revealed the differentiation of the P1 pocket in the HLA-DP family. These results provide the essential structural basis for understanding the diversification of the ligand-binding specificities in the HLA-DP family, toward innovative pharmaceutical research for patients with hay fever.

## Materials and Methods

### Cloning, expression, and purification

The gene encoding the signal sequence and residues 1–181 of the HLA-DP5α chain was cloned into the baculovirus transfer vector pFastBacDual (Life Technologies), as a fusion with the C-terminal tobacco etch virus (TEV) protease cleavage site and a His tag. The gene encoding residues 4–189 of the HLA-DP5β chain was cloned into the resulting vector, as a fusion with the gp67 signal sequence followed by the nine-amino-acid residues (KVTVAFNQF) of the Cry j 1 peptide and the linker sequence (GGSLVPRGSGGGGS) at its N-terminus, as well as the TEV protease cleavage site and FLAG tag at its C-terminus. The baculovirus for the His-tagged HLA-DP5α and FLAG-tagged Cry j 1–HLA-DP5β production was created using the BAC-to-BAC Baculovirus Expression System (Invitrogen). *Spodoptera frugiperda* cells ($5 \times 10^5$ cells/ml), derived from expresSF+® Insect Cells (Protein Sciences), were cultured in Sf-900™ III SFM (Life Technologies) and infected with the viral stock at a multiplicity of infection of 0.2. After 20 h at 27 °C in suspension culture (125 rpm), the cells were pelleted and resuspended in an equal volume of the medium and were continuously cultured at 19 °C in suspension for 5 days. The heterodimer HLA-DP5•Cry j 1(9-mer) was purified from the culture supernatants by immobilized ANTI-FLAG® M2 Affinity Gel (Sigma) and then the C-terminal tag of the heterodimer in the eluate was removed by an overnight treatment with TEV protease at 4 °C. Seven residues (GSSGSSG) from the tag remain at the C-terminus because of the location of the TEV cleavage site. The heterodimer was further purified by size-exclusion

chromatography (Superdex 200 HR 10/30; GE Healthcare) and eluted with 20 mM Tris–HCl buffer (pH 8.0) containing 150 mM NaCl. The appropriate fractions were collected according to the SDS-PAGE analysis.

### Analytical ultracentrifugation

All of the analytical ultracentrifugation experiments were performed at 4 °C, using an An-50 Ti rotor and a Beckman Optima XL-I analytical ultracentrifuge. Absorbance scans were recorded at 280 nm. The sample buffer was 20 mM Tris–HCl, pH 8.0, containing 150 mM NaCl. The solvent density and the protein partial specific volume ($\bar{v}$) were estimated using the program SEDNTERP[†]. The sedimentation coefficient was determined from sedimentation velocity experiments, performed at a rotor speed of 40,000 rpm. The concentrations of the protein samples were 0.32 and 0.16 mg/ml. The data were analyzed with the program SEDFIT [32]. For the sedimentation equilibrium experiments, protein samples at three different concentrations (0.40, 0.27, and 0.13 mg/ml) were centrifuged at rotor speeds of 6000, 7500, 9000, 10,500, and 12,000 rpm until the sedimentation–diffusion equilibrium was reached (16 h). The equilibrium data were fitted using the manufacturer's software (Beckman XL-A/XL-I Data Analysis Software ver. 6.03).

### Crystallization and X-ray data collection

The preliminary crystals of the HLA-DP5•Cry j 1(9-mer) complex were obtained by initial crystallization screening, using the 96-well sitting-drop vapor diffusion method (Hampton Research). The crystals of the HLA-DP5•Cry j 1(9-mer) complex used for structure determination were obtained by the sitting-drop vapor diffusion method, by mixing the protein solution (0.7 mg/ml) with an equal volume of the reservoir solution [24% (w/v) polyethylene glycol 3350 and 0.2 M ammonium nitrate] and incubating the mixture at 20 °C. Plate-like crystals grew to average dimensions of 0.5 mm × 0.2 mm × 0.01 mm within 2 weeks. A single crystal of HLA-DP5•Cry j 1(9-mer) was coated with its reservoir solution, containing 22.5% polyethylene glycol 400 as cryoprotectant, and was flash-cooled in liquid nitrogen. The native diffraction data of HLA-DP5•Cry j 1(9-mer) were collected at −173 °C at a single wavelength at X06SA, Swiss Light Source, and were recorded on a MARmosaic 225 CCD detector (Rayonix, USA). All of the HLA-DP5•Cry j 1(9-mer) diffraction data were processed with the XDS program [33]. The crystallographic data and the data collection statistics of HLA-DP5•Cry j 1(9-mer) are provided in Table 1.

### Structure determination and refinement

We solved the structure of the HLA-DP5•Cry j 1(9-mer) heterodimer by molecular replacement with PHASER [34], using the reported HLA-DP2 structure (PDB accession code: 3LQZ), with pDRA omitted, as a search model. This solution was subjected to one round of simulated annealing refinement in PHENIX [35]. The initial maps showed additional density in the peptide-binding groove, which indicated the binding site for Cry j 1(9-mer). The HLA-DP5•Cry j 1(9-mer) model was subsequently completed by manual rebuilding in Coot [36] and rigid-body refinement in PHENIX, with a single *B*-factor per domain, using local non-crystallographic symmetry restraints throughout. The last round of refinement was performed without non-crystallographic symmetry. There are four HLA-DP5•Cry j 1(9-mer) complexes in the asymmetric unit. Refinement statistics are provided in Table 1. The programs PROCHECK [37] and MolProbity [38] were used to assess the geometry of the final model. Ramachandran statistics are as follows [favored/disallowed (%)]: HLA-DP5•Cry j 1(9-mer), 98/0.1. Alignments were calculated using CLUSTAL W [39]. Figures were produced using PyMOL[‡].

### *In vitro* protein binding assay

The DNA fragments encoding the full-length ectodomain of HLA-DP5α (residues 1–181) and that of HLA-DP5β (residues 4–189) as an N-terminal fusion with the nine-amino-acid residue Cry j 1 peptide (KVTVAFNQF) were cloned into the TA vector pCR2.1TOPO (Invitrogen). HLA-DP5α and HLA-DP5β are fusion proteins containing C-terminal histidine and FLAG tags, respectively, following the TEV protease cleavage site. The Kp1E, Tp3Y, Np7Q, Qp8E, and Fp9A mutants of Cry j 1(9-mer) were prepared by site-directed mutagenesis, using a QuikChange Site-Directed Mutagenesis kit (Stratagene). These variants were synthesized using the small scale dialysis mode of the *Escherichia coli* cell-free reaction [40,41] in the presence of disulfide isomerase and GSH/GSSG. Equal amounts of HLA-DP5 in complex with Cry j 1(WT) and Cry j 1(Mutants) were incubated with Ni-NTA agarose (Qiagen) beads. The beads were washed 10 times with washing buffer [20 mM Tris–HCl buffer (pH 8.0), containing 150 mM NaCl and 20 mM imidazole]. The bound proteins were eluted with 20 mM Tris–HCl buffer (pH 8.0), containing 150 mM NaCl and 500 mM imidazole, resolved by SDS-PAGE and stained by Coomassie Brilliant Blue. Simultaneously, equal amounts of these variants were incubated with ANTI-FLAG® M2 Affinity Gel (Sigma) beads. The beads were washed five times with washing buffer [20 mM Tris–HCl buffer (pH 8.0), containing 150 mM NaCl and 1 mM ethylenediaminetetraacetic acid]. The bound proteins were eluted with 20 mM Tris–HCl buffer (pH 8.0), containing 150 mM NaCl, 1 mM ethylenediaminetetraacetic acid, and 0.1 mg/ml 3× FLAG® Peptide (Sigma), and the fractions were analyzed by SDS-PAGE and immunoblotted with an ANTI-FLAG® M2 Monoclonal Antibody (Sigma). Immunoblotting images were obtained using a Luminescent Image Analyzer (LAS-4000; GE Healthcare).

### Phylogenic analysis

The NJ tree [42] of synonymous substitutions was constructed by using a program implemented in MEGA5 [43]. On the NJ tree, amino acid substitutions within the PBRs of the DPα and DPβ chains were manually placed parsimoniously. For *DPA1*, *DRA1* sequences were used as outgroups, but for *DPB1*, outgroup sequences were not used. Instead, the root was placed on an inter-nodal branch of the DP2 and DP5 groups.

**Accession number**

The atomic coordinates and structure factors of the HLA-DP5 • Cry j 1(9-mer) complex have been deposited in the PDB, with the accession code 3WEX.

## Acknowledgements

We would like to thank M. Aoki, M. Nishimoto, C. Mishima-Tsumagari, F. Konishi, and M. Kawazoe for technical assistance. We are grateful to the beamline staff at the X06SA of Swiss Light Source for assistance in data collection. This work was supported by a Grant-in-Aid for Scientific Research on Innovative Areas (Grant Number 22133004), the Japan Society for the Promotion of Science, and the Targeted Proteins Research Program of the Ministry of Education, Culture, Sports, Science and Technology of Japan.

**Competing Financial Interests:** The authors declare no competing financial interests.

## Appendix A. Supplementary data

Supplementary data to this article can be found online at http://dx.doi.org/10.1016/j.jmb.2014.06.020.

*Received 25 April 2014;*
*Received in revised form 26 June 2014;*
*Accepted 27 June 2014*
Available online 11 July 2014

***Keywords:***
HLA-DP5;
Cry j 1;
cedar pollen;
X-ray crystallography;
evolutionary analysis

† http://www.jphilo.mailway.com.
‡ http://www.pymol.org/.

***Abbreviations used:***
IgEimmunoglobulin E; HLAhuman leukocyte antigen; PBRpeptide-binding region; TEVtobacco etch virus.

## References

[1] Bhalla PL. Genetic engineering of pollen allergens for hayfever immunotherapy. Expert Rev Vaccines 2003;2:75–84.
[2] von Mutius E, Vercelli D. Farm living: effects on childhood asthma and allergy. Nat Rev 2010;10:861–8.
[3] Greiner AN, Hellings PW, Rotiroti G, Scadding GK. Allergic rhinitis. Lancet 2011;378:2112–22.
[4] Ferreira F, Hawranek T, Gruber P, Wopfner N, Mari A. Allergic cross-reactivity: from gene to the clinic. Allergy 2004;59:243–67.
[5] Horiguchi S, Saito Y. Discovery of Japanese cedar pollinosis in Nikko, Ibaraki Prefecture. Arerugi 1964;13:16–8.
[6] Kaneko Y, Motohashi Y, Nakamura H, Endo T, Eboshida A. Increasing prevalence of Japanese cedar pollinosis: a meta-regression analysis. Int Arch Allergy Immunol 2005;136:365–71.
[7] Sone T, Komiyama N, Shimizu K, Kusakabe T, Morikubo K, Kino K. Cloning and sequencing of cDNA coding for Cry j I, a major allergen of Japanese cedar pollen. Biochem Biophys Res Commun 1994;199:619–25.
[8] Komiyama N, Sone T, Shimizu K, Morikubo K, Kino K. cDNA cloning and expression of Cry j II the second major allergen of Japanese cedar pollen. Biochem Biophys Res Commun 1994;201:1021–8.
[9] Fujimura T, Futamura N, Midoro-Horiuti T, Togawa A, Goldblum RM, Yasueda H, et al. Isolation and characterization of native Cry j 3 from Japanese cedar (*Cryptomeria japonica*) pollen. Allergy 2007;62:547–53.
[10] Honda K, Matsushita S, Yasuda N, Juji T, Sasazuki T, Uemura T. Segregation analysis of IgE responses to *Cryptomeria japonica* pollen antigen *in vivo*. Eur Arch Otorhinolaryngol 1994;251:S68–72.
[11] Okano M. Antigenicity and allergenicity of pollens, especially in Japanese cedar pollinosis. Prog Med 2000;20: 2458–63.
[12] Taniguchi Y, Ono A, Sawatani M, Nanba M, Kohno K, Usui M, et al. Cry j I, a major allergen of Japanese cedar pollen, has pectate lyase enzyme activity. Allergy 1995;50:90–3.
[13] Ohtsuki T, Taniguchi Y, Kohno K, Fukuda S, Usui M, Kurimoto M. Cry j 2, a major allergen of Japanese cedar pollen, shows polymethylgalacturonase activity. Allergy 1995;50:483–8.
[14] Gould HJ, Sutton BJ. IgE in allergy and asthma today. Nat Rev 2008;8:205–17.
[15] Neefjes J, Jongsma ML, Paul P, Bakke O. Towards a systems understanding of MHC class I and MHC class II antigen presentation. Nat Rev 2011;11:823–36.
[16] Carroll MC, Katzman P, Alicot EM, Koller BH, Geraghty DE, Orr HT, et al. Linkage map of the human major histocompatibility complex including the tumor necrosis factor genes. Proc Natl Acad Sci USA 1987;84:8535–9.
[17] Wake CT. Molecular biology of the HLA class I and class II genes. Mol Biol Med 1986;3:1–11.
[18] Kim CY, Quarsten H, Bergseng E, Khosla C, Sollid LM. Structural basis for HLA-DQ2-mediated presentation of gluten epitopes in celiac disease. Proc Natl Acad Sci USA 2004;101:4175–9.
[19] Tollefsen S, Hotta K, Chen X, Simonsen B, Swaminathan K, Mathews II, et al. Structural and functional studies of trans-encoded HLA-DQ2.3 (DQA1*03:01/DQB1*02:01) protein molecule. J Biol Chem 2012;287:13611–9.
[20] Henderson KN, Tye-Din JA, Reid HH, Chen Z, Borg NA, Beissbarth T, et al. A structural and immunological basis for the role of human leukocyte antigen DQ8 in celiac disease. Immunity 2007;27:23–34.
[21] Broughton SE, Petersen J, Theodossis A, Scally SW, Loh KL, Thompson A, et al. Biased T cell receptor usage directed against human leukocyte antigen DQ8-restricted gliadin peptides is associated with celiac disease. Immunity 2012;37:611–21.
[22] Hori T, Kamikawaji N, Kimura A, Sone T, Komiyama N, Komiyama S, et al. Japanese cedar pollinosis and HLA-DP5. Tissue Antigens 1996;47:485–91.

[23] Sone T, Morikubo K, Miyahara M, Komiyama N, Shimizu K, Tsunoo H, et al. T cell epitopes in Japanese cedar (*Cryptomeria japonica*) pollen allergens: choice of major T cell epitopes in Cry j 1 and Cry j 2 toward design of the peptide-based immunotherapeutics for the management of Japanese cedar pollinosis. J Immunol 1998;161:448–57.
[24] Sone T, Morikubo K, Shimizu K, Komiyama N, Tsunoo H, Kino K. Peptide specificity, HLA class II restriction, and T-cell subsets of the T-cell clones specific to either Cry j 1 or Cry j 2, the major allergens of Japanese cedar (*Cryptomeria japonica*) pollen. Int Arch Allergy Immunol 1999;119:185–96.
[25] Dai S, Murphy GA, Crawford F, Mack DG, Falta MT, Marrack P, et al. Crystal structure of HLA-DP2 and implications for chronic beryllium disease. Proc Natl Acad Sci USA 2010;107:7425–30.
[26] Painter CA, Stern LJ. Conformational variation in structures of classical and non-classical MHCII proteins and functional implications. Immunol Rev 2012;250:144–57.
[27] Hollenbach JA, Madbouly A, Gragert L, Vierra-Green C, Flesch S, Spellman S, et al. A combined DPA1~DPB1 amino acid epitope is the primary unit of selection on the HLA-DP heterodimer. Immunogenetics 2012;64:559–69.
[28] Baker BM, Scott DR, Blevins SJ, Hawse WF. Structural and dynamic control of T-cell receptor specificity, cross-reactivity, and binding mechanism. Immunol Rev 2012;250:10–31.
[29] Diaz G, Canas B, Vazquez J, Nombela C, Arroyo J. Characterization of natural peptide ligands from HLA-DP2: new insights into HLA-DP peptide-binding motifs. Immunogenetics 2005;56:754–9.
[30] Hansen BE, Nielsen CH, Madsen HO, Ryder LP, Jakobsen BK, Svejgaard A. The HLA-DP2 protein binds the immunodominant epitope from myelin basic protein, MBP85-99, with high affinity. Tissue Antigens 2011;77:229–34.
[31] Dai S, Falta MT, Bowerman NA, McKee AS, Fontenot AP. T cell recognition of beryllium. Curr Opin Immunol 2013;25:775–80.
[32] Schuck P. Size-distribution analysis of macromolecules by sedimentation velocity ultracentrifugation and Lamm equation modeling. Biophys J 2000;78:1606–19.
[33] Kabsch W. XDS. Acta Crystallogr 2010;66:125–32.
[34] McCoy AJ, Grosse-Kunstleve RW, Adams PD, Winn MD, Storoni LC, Read RJ. Phaser crystallographic software. J Appl Crystallogr 2007;40:658–74.
[35] Adams PD, Afonine PV, Bunkoczi G, Chen VB, Davis IW, Echols N, et al. PHENIX: a comprehensive Python-based system for macromolecular structure solution. Acta Crystallogr 2010;66:213–21.
[36] Emsley P, Cowtan K. Coot: model-building tools for molecular graphics. Acta Crystallogr 2004;60:2126–32.
[37] Laskowski R, MacArthur M, Moss D, Thornton J. PROCHECK: a program to check the stereochemical quality of protein structures. J Appl Crystallogr 1993;26:283–91.
[38] Davis IW, Leaver-Fay A, Chen VB, Block JN, Kapral GJ, Wang X, et al. MolProbity: all-atom contacts and structure validation for proteins and nucleic acids. Nucleic Acids Res 2007;35:W375–83.
[39] Thompson JD, Higgins DG, Gibson TJ. CLUSTAL W: improving the sensitivity of progressive multiple sequence alignment through sequence weighting, position-specific gap penalties and weight matrix choice. Nucleic Acids Res 1994;22:4673–80.
[40] Kigawa T, Yabuki T, Matsuda N, Matsuda T, Nakajima R, Tanaka A, et al. Preparation of *Escherichia coli* cell extract for highly productive cell-free protein expression. J Struct Funct Genomics 2004;5:63–8.
[41] Kigawa T, Matsuda T, Yabuki T, Yokoyama S. Bacterial cell-free system for highly efficient protein synthesis. In: Spirin AS, Swartz JR, editors. Cell-Free Protein Synthesis. Weinheim: Wiley-VCH; 2007. p. 83–97.
[42] Saitou N, Nei M. The neighbor-joining method: a new method for reconstructing phylogenetic trees. Mol Biol Evol 1987;4:406–25.
[43] Tamura K, Peterson D, Peterson N, Stecher G, Nei M, Kumar S. MEGA5: molecular evolutionary genetics analysis using maximum likelihood, evolutionary distance, and maximum parsimony methods. Mol Biol Evol 2011;28:2731–9.

Bioinformatics Advance Access published October 13, 2014

BIOINFORMATICS APPLICATIONS NOTE 2014, pages 1–3
doi:10.1093/bioinformatics/btu644

Genome analysis

Advance Access publication September 25, 2014

# PINBPA: Cytoscape app for network analysis of GWAS data

Lili Wang[1], Takuya Matsushita[2], Lohith Madireddy[2], Parvin Mousavi[1] and Sergio E. Baranzini[2,*]

[1]School of Computing, Queen's University, 25 Union Street, Goodwin Hall, Kingston, Ontario K7L 3N6, Canada and [2]Department of Neurology, University of California San Francisco, 675 Nelson Rising Lane, Room 215, San Francisco, CA 94158, USA

Associate Editor: John Hancock

## ABSTRACT

**Summary:** Protein interaction network-based pathway analysis (PINBPA) for genome-wide association studies (GWAS) has been developed as a Cytoscape app, to enable analysis of GWAS data in a network fashion. Users can easily import GWAS summary-level data, draw Manhattan plots, define blocks, prioritize genes with random walk with restart, detect enriched subnetworks and test the significance of subnetworks via a user-friendly interface.

**Availability and implementation:** PINBPA app is freely available in Cytoscape app store.

**Contact:** pmousavi@cs.queensu.ca and sebaran@cgl.ucsf.edu

**Supplementary information:** Supplementary data are available at *Bioinformatics* online.

Received on August 8, 2014; revised on September 18, 2014; accepted on September 22, 2014

## 1 INTRODUCTION

Genome-wide association studies (GWAS) continue to be a widely used approach to detect genetic associations with a phenotype of interest in well-defined populations. As of September 15, 2014, almost 2000 publications have reported associations of >13 000 single-nucleotide polymorphisms (SNPs) with close to 200 phenotypes in the GWAS catalog (Welter *et al.*, 2014). The successful record of this genomic mapping strategy includes the identification of dozens or even hundreds of susceptibility alleles in common diseases, such as multiple sclerosis (MS), type 1 and type 2 diabetes, lymphomas, leukemias and metabolic disorders. Despite the unquestionable utility of this method, most of the data generated by GWAS are neglected because of the heavy emphasis devoted to eliminate false discoveries (type I error). Typically, a stringent threshold ($P\text{-}value < 5 \times 10^{-8}$) is applied to minimize type I error, thus inevitably increasing the proportion of false-negative results (type II error). Although this is a necessary tactic to effectively evaluate studies testing up to millions of markers individually, a number of methods that analyze groups of markers simultaneously (thus potentially increasing statistical power) have recently emerged (Huang Da *et al.*, 2009; Khatri *et al.*, 2012; Lee *et al.*, 2012; Wang *et al.*, 2007; Yaspan *et al.*, 2011). These approaches, collectively known as pathway analysis, aim at identifying functional relationships among associated signals. Given that susceptibility to complex human diseases is likely a result of genes operating as part of functional modules rather than individual effects (Lage *et al.*, 2007), pathway analysis methods hold promise in discovering additional associations from existing GWAS data.

The most recent class of pathway analysis methods is network based, and they largely overcome the assumptions of independence and preselection of reference database that limited its predecessors. Network-based analyses commonly use a scaffold of protein interactions to build connections between gene products, where nodes represent proteins and edges represent physical or functional interactions between pairs of proteins. Rather than focusing on individual markers, network-based analysis methods take into account multiple loci in the context of molecular pathways. Owing to this critical feature, these methods can afford to use sub genome-wide statistical significance and yet increase the power to detect new associations and functional relationships between genes in complex traits. Several network-based methods have been proposed to identify active modules (subnetworks) in a given network, such as DAPPLE (Rossin *et al.*, 2011), dmGWAS (Jia *et al.*, 2011) and NIMMI (Akula *et al.*, 2011).

The original protein interaction network-based pathway analysis (PINBPA) method was first developed in the context of MS research (Baranzini *et al.*, 2009) and most recently used to successfully identify novel associations by the International MS Genetics Consortium (International Multiple Sclerosis Genetics Consortium, 2013). In this article, we introduce the PINBPA app for Cytoscape (Shannon *et al.*, 2003).

## 2 IMPLEMENTATION AND FEATURES

PINBPA has been implemented as an app for Cytoscape 3.0 and later versions using Java. Additionally, R scripts are called via Rserve inside Cytoscape for plotting.

Like many other pathway analysis methods, PINBPA requires gene-level summary statistics (*P*-values), as those generated by the popular tool VEGAS (Liu *et al.*, 2010). As shown in Figure 1, the PINBPA app directly reads the VEGAS output as input file (but other formats are also possible), and has six features: (i) generates a gene-wise Manhattan plot of the GWAS; (ii) sorts all genes by their genomic coordinates and defines association blocks at any user-defined threshold ($P\text{-}value < 0.05$ by default); (iii) annotates the user-selected PPI network with imported gene-wise GWAS *P*-values; (iv) generates a subnetwork of only significant genes (first-order networks) exceeding a user-defined threshold, and tests the statistical significance of the sub-networks using random permutations; (v) runs network smoothing (an optional gene prioritization scheme) using a

*To whom correspondence should be addressed.

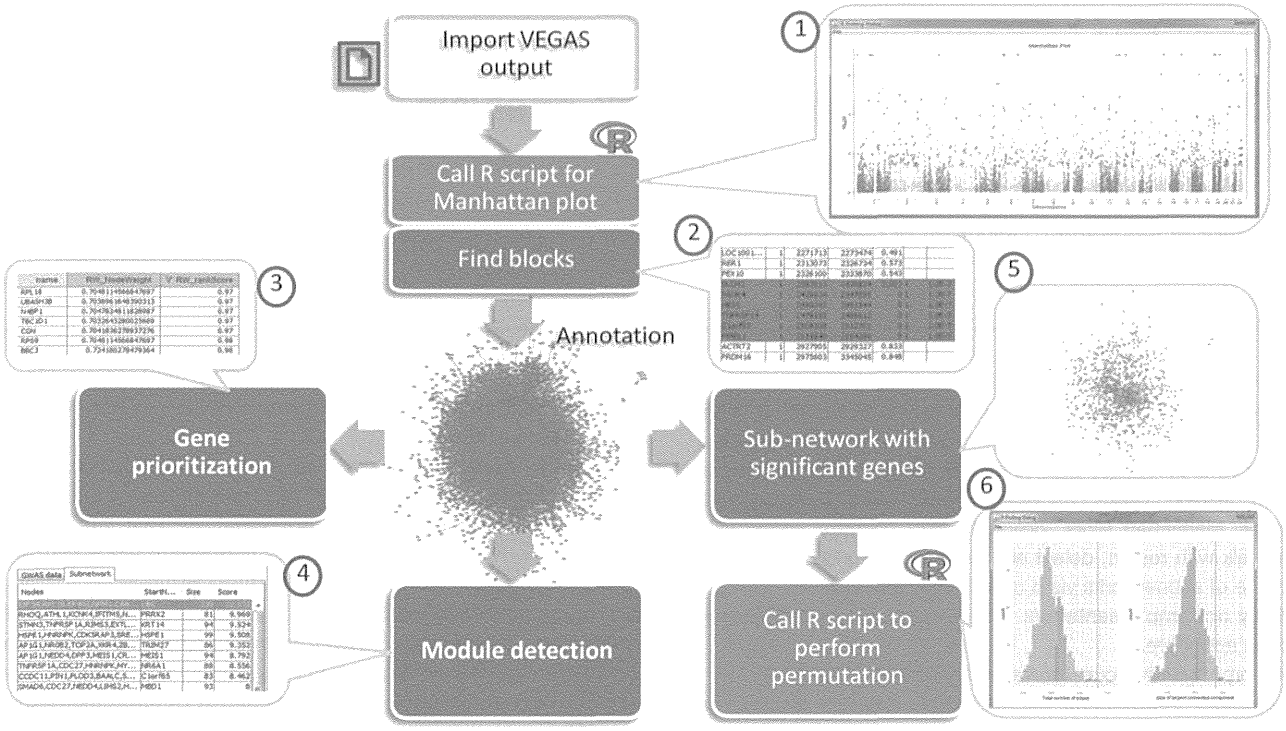


**Fig. 1.** Workflow of PINBPA. The blue blocks denote functions implemented in java, and the orange blocks denote functions calling R scripts

random walk with restart algorithm (Kohler *et al.*, 2008); and (vi) detects subnetworks enriched in significant genes using either unweighted (Ideker *et al.*, 2002) or weighted z-scores (Whitlock, 2005). The network z-score is adjusted using 1000 permutations and then a greedy algorithm (Supplementary File) is applied to search for the n optimal subnetworks.

## 3 DISCUSSION

PINBPA is the first Cytoscape app designed for network analysis of GWAS data. Through a user-friendly interface, the PINBPA app enables genomic researchers and biologists with no computational expertise to run a powerful and otherwise complex analytical pipeline. PINBPA is flexible in many ways. First, it enables the use of any network as scaffold for subsequent analysis. For example, a user may choose to run PINBPA using a smaller but high confidence PIN, or a larger network, including computationally predicted interactions. Additionally, other networks such as metabolic, gene co-expression or text mining can be used. Second, while direct import from VEGAS is available, any method can be used to convert SNP-level and gene-level *P*-values. Third, the user can select the significance threshold to define association blocks. Although some experimentation may be needed, this significance threshold is typically related to the power of the GWAS in question (the larger the GWAS, the more relaxed the *P*-value for block definition). Fourth, significant (first-order) networks can be generated at any user-selected statistical threshold. Fifth, an optional network smoothing step allows the user to weight the most significant associations differently. Finally, the size and the significance of enriched networks generated by the greedy algorithm can also be selected, thus providing maximal control over the final output.

In summary, the Cytoscape PINBPA app offers a simple interface to perform a complex set of analyses and can be used under a wide variety of scenarios, thus empowering genomic scientists to conduct post-GWAS analysis in a streamlined, rigorous and reproducible fashion.

*Funding*: S.E.B. is a Harry Weaver Neuroscience scholar of the National MS Society.

*Conflict of interest*: none declared.

## REFERENCES

Akula,N. *et al.* (2011) A network-based approach to prioritize results from genome-wide association studies. *PLoS One*, **6**, E24220.

Baranzini,S.E. *et al.* (2009) Pathway and network-based analysis of genome-wide association studies in multiple sclerosis. *Hum. Mol. Genet.*, **18**, 2078–2090.

Huang Da,W. *et al.* (2009) Bioinformatics enrichment tools: paths toward the comprehensive functional analysis of large gene lists. *Nucleic Acids Res.*, **37**, 1–13.

Ideker,T. *et al.* (2002) Discovering regulatory and signalling circuits in molecular interaction networks. *Bioinformatics*, **18** (**Suppl. 1**), S233–S240.

International Multiple Sclerosis Genetics Consortium. (2013) Network-based multiple sclerosis pathway analysis with gwas data from 15,000 cases and 30,000 controls. *Am. J. Hum. Genet.*, **92**, 854–865.

Jia,P. *et al.* (2011) dmGWAS: dense module searching for genome-wide association studies in protein-protein interaction networks. *Bioinformatics*, **27**, 95–102.

Khatri,P. *et al.* (2012) Ten years of pathway analysis: current approaches and outstanding challenges. *PLoS Comput. Biol.*, **8**, e1002375.

Kohler,S. *et al.* (2008) Walking the interactome for prioritization of candidate disease genes. *Am. J. Hum. Genet.*, **82**, 949–958.

Lage,K. *et al.* (2007) A human phenome-interactome network of protein complexes implicated in genetic disorders. *Nat. Biotechnol.*, **25**, 309–316.

Lee,P.H. *et al.* (2012) INRICH: interval-based enrichment analysis for genome-wide association studies. *Bioinformatics*, **28**, 1797–1799.

Liu,J.Z. *et al.* (2010) A versatile gene-based test for genome-wide association studies. *Am. J. Hum. Genet.*, **87**, 139–145.

Rossin,E.J. *et al.* (2011) Proteins encoded in genomic regions associated with immune-mediated disease physically interact and suggest underlying biology. *PLos Genet.*, **7**, e1001273.

Shannon,P. *et al.* (2003) Cytoscape: a software environment for integrated models of biomolecular interaction networks. *Genome Res.*, **13**, 2498–2504.

Wang,K. *et al.* (2007) Pathway-based approaches for analysis of genomewide association studies. *Am. J. Hum. Genet.*, **81**, 1278–1283.

Welter,D. *et al.* (2014) The NHGRI GWAS catalog, a curated resource of SNP-trait associations. *Nucleic Acids Res.*, **42**, D1001–D1006.

Whitlock,M.C. (2005) Combining probability from independent tests: the weighted z-method is superior to fisher's approach. *J. Evol. Biol.*, **18**, 1368–1373.

Yaspan,B.L. *et al.* (2011) Genetic analysis of biological pathway data through genomic randomization. *Hum. Genet.*, **129**, 563–571.

Clinical & Experimental
Neuroimmunology

Clinical and Experimental Neuroimmunology 5 (2014) 279–280

COMMENTARY

# Autoimmune regulator gene, Aire, and its relevance to central tolerance against myelin proteins

Hirofumi Ochi

Department of Neurology, Ehime University Graduate School of Medicine, Ehime, Japan

**Correspondence**
Hirofumi Ochi, MD, PhD, Department of Neurology, Ehime University Graduate School of Medicine, 454 Shitsukawa, Toon, Ehime 791-0295, Japan.
Tel: +81-89-960-5851
Fax: +81-89-960-5852
Email: hochi@m.ehime-u.ac.jp

Received: 8 August 2014; accepted: 11 August 2014.

**Abstract**

The autoimmune regulator (Aire) is a key transcription factor that promotes promiscuous expression of tissue-specific antigens by medullary thymic epithelial cells (mTEC), and mediates a role in negative selection of autoreactive T cells. Tagawa et al. reported the central role of Aire in establishing central tolerance to myelin antigen, and its deficiency resulted in spontaneous autoreactivity against central nervous system myelin antigen. The role of mTEC-dependent tolerance in multiple sclerosis must await further study.

Multiple sclerosis (MS) is a chronic debilitating autoimmune inflammatory and neurodegenerative disorder of the central nervous system (CNS) characterized by the presence of inflammation, myelin damage and axonal loss. It has long been considered that myelin-reactive T cells play a crucial role in the autoimmune cascade during disease initiation and progression.

Many tissue-specific antigens (TSA) are known to be expressed in the thymus primarily by medullary thymic epithelial cells (mTEC).[1] The pool of these mTEC-expressed TSA covers most of the putative autoantigens in both mice and human autoimmunity, and this pool is considered to be crucial for negative selection of developing thymocytes with a high avidity for autoantigens.[2] Thus, sufficient display of TSA in mTEC is required to limit the escape of autoreactive T cells to the periphery, leading to autoimmunity unless controlled by peripheral regulatory cells.

Myelin proteolipid protein (PLP) is the main component of CNS myelin. There are two isoforms resulting from different mRNA splicing; PLP is the longer isoform and DM20 is the shorter isoform that lacks residues 116–150 of the full-length protein. Although both PLP and DM20 are predominantly expressed in the CNS, DM20 is the dominant isoform expressed in non-CNS tissues, thus the predominant form of PLP expressed in the thymus is a shorter splice variant DM20.[3] Consequently, only thymocytes that recognize epitopes in DM20 would be expected to be eliminated within the thymus. Indeed, analysis of the T-cell repertoire to PLP in PLP-deficient C57BL/6 mice shows T cells that respond to epitopes in DM20 undergo negative selection.[3] SJL mice are highly susceptible to the induction of experimental autoimmune encephalomyelitis (EAE), and the immunodominant epitope of this strain is PLP139-151, which is not contained in DM20. This suggests that the predominant expression of DM20 in the thymus is responsible for the lack of negative selection of T cells reactive to PLP139-151. In addition, re-expression of PLP139-151 in the embryonic thymus results in a reduced frequency of PLP139-151-reactive T cells in the periphery and the loss of immunodominance of this epitope.[4]

Autoimmune regulatory (Aire) gene is a transcription factor that mediates a role in negative selection of autoreactive T cells in part by controlling the expression of numerous TSA in mTEC.[1] Indeed, Aire deficiency causes downregulation of more than 1000 TSA in the mTEC, resulting in impaired central tolerance.[5] In addition to its function in regulating the transcription of TSA in the thymus, Aire is also shown to control antigen processing and/or presentation, chemokine and cytokine production, and mTEC maturation.[1]

Tagawa et al.[6] reported the low levels of thymic DM20 expression in Aire-deficient C57BL/6 mice was associated with the increased susceptibility to

EAE, and the encephalitogenic PLP178-191 is linked to Aire regulation. In addition, spontaneous autoreactivity in response to PLP178-191 was enhanced in Aire-deficient C57BL/6 mice, suggesting the potentially spontaneous CNS autoimmunity in aged Aire-deficient C57BL/6 mice. Although other encephalitogenic antigen myelin oligodendrocyte glycoprotein is also reported to be linked to Aire regulation, the reduction of myelin oligodendrocyte glycoprotein mRNA expression in the thymus was not observed in this study.[7,8] So far, the reason of these conflicting results still remains obscure.

Loss-of-function mutations in the Aire gene in humans cause a rare autosomal recessive autoimmune disease, autoimmune polyendocrinopathy-candidiasis-ectodermal dystrophy (APECED). Although the phenotype of Aire-deficient mice is considerably milder than that of human APECED, both conditions are characterized by autoimmune infiltrates in multiple organs and autoantibodies to multiple organ-specific antigens. Thus, organ-specific autoimmune conditions in Aire-deficient humans and animals are considered to be linked, at least in part to a failure in the appropriate thymic expression of selective autoantigen that is controlled by Aire. α-Subunit of the muscle acethylcholine receptor is the main target of pathogenic autoantibodies in myasthenia gravis (MG), and has been shown to be controlled by Aire. Although MG is not a feature of APECED, the reduced expression of *CHRNA1* in mTEC, which encodes the α-subunit of the muscle acethylcholine receptor, is reported to be associated with the onset of MG.[9] These imply that the onset of autoimmunity in humans could be related to impaired expression of TSA in mTEC; however, dysregulation of mTEC-dependent tolerance is not the only mechanism behind Aire-induced T-cell tolerance. Actually, Aire-deficient mice developed a Sjögren's syndrome-like autoimmune reaction against α-fodrin, which is expressed normally in the thymus.[10] It is tempting to speculate that other additional factors, such as peripheral immunological and environmental factors, might be involved in the pathogenesis of the autoimmune condition in Aire-deficient humans and animals.

Intrathymic expression of PLP in humans is also restricted to the DM20 isoform. Tagawa et al.[6] showed for the first time that PLP was under Aire control; however, MS is not a feature of APECED. Thus, the role of mTEC-dependent tolerance in MS needs to be further investigated.

## References


1. Laan M, Peterson P. The many faces of aire in central tolerance. *Front Immunol.* 2013; **4**: 326.
2. Kyewski B, Derbinski J. Self-representation in the thymus: an extended view. *Nat Rev Immunol.* 2004; **4**: 688–98.
3. Klein L, Klugmann M, Nave KA, Tuohy VK, Kyewski B. Shaping of the autoreactive T-cell repertoire by a splice variant of self protein expressed in thymic epithelial cells. *Nat Med.* 2000; **6**: 56–61.
4. Anderson AC, Nicholson LB, Legge KL, Turchin V, Zaghouani H, Kuchroo VK. High frequency of autoreactive myelin proteolipid protein-specific T cells in the periphery of naive mice: mechanisms of selection of the self-reactive repertoire. *J Exp Med.* 2000; **191**: 761–70.
5. Liston A, Lesage S, Wilson J, Peltonen L, Goodnow CC. Aire regulates negative selection of organ-specific T cells. *Nat Immunol.* 2003; **4**: 350–4.
6. Tagawa A, Aranami T, Matsumoto M, Yamamura T. Autoimmune regulator gene, *Aire*, is involved in central tolerance to the DM20 isoform of proteolipid protein and the prevention of autoimmune inflammation. *Clin Exp Neuroimmunol.* 2014; **5**: 304–14.
7. Ko HJ, Kinkel SA, Hubert FX, et al. Transplantation of autoimmune regulator-encoding bone marrow cells delays the onset of experimental autoimmune encephalomyelitis. *Eur J Immunol.* 2010; **40**: 3499–509.
8. Aharoni R, Aricha R, Eilam R, et al. Age dependent course of EAE in Aire-/- mice. *J Neuroimmunol.* 2013; **262**: 27–34.
9. Giraud M, Taubert R, Vandiedonck C, et al. An IRF8-binding promoter variant and AIRE control CHRNA1 promiscuous expression in thymus. *Nature.* 2007; **448**: 934–7.
10. Kuroda N, Mitani T, Takeda N, et al. Development of autoimmunity against transcriptionally unrepressed target antigen in the thymus of Aire-deficient mice. *J Immunol.* 2005; **174**: 1862–70.

Clinical & Experimental Neuroimmunology

Clinical and Experimental Neuroimmunology 5 (2014) 321–327

ORIGINAL ARTICLE

# Distinct cytokine and T helper cell profiles between patients with multiple sclerosis who had or had not received interferon-beta

Hikaru Doi,[1] Zi-Ye Song,[1] Satoshi Yoshimura,[1] Takahisa Tateishi,[1] Tomomi Yonekawa,[1] Ryo Yamasaki,[2] Hiroyuki Murai,[1] Takuya Matsushita[1] and Jun-ichi Kira[1]

[1]Department of Neurology, Neurological Institute, Graduate School of Medical Sciences, Kyushu University, Fukuoka, Japan, [2]Department of Neurological Therapeutics, Neurological Institute, Graduate School of Medical Sciences, Kyushu University, Fukuoka, Japan

**Keywords**
flow cytometry; fluorescence bead-based immunoassay; interferon-β; interleukin 17; interleukin 9; multiple sclerosis; T helper 17 cell; T helper 9 cell

**Correspondence**
Jun-ichi Kira, MD, PhD, Department of Neurology, Neurological Institute, Graduate School of Medical Sciences, Kyushu University, 3-1-1 Maidashi, Higashi-ku, Fukuoka 812-8582, Japan.
Tel: +81-92-642-5340
Fax: +81-92-642-5352
Email: kira@neuro.med.kyushu-u.ac.jp

Received: 4 April 2014; revised: 9 June 2014; accepted: 10 June 2014.

## Abstract

**Objectives** Multiple sclerosis (MS) is an inflammatory demyelinating disease of the central nervous system, and is generally considered to be mediated by T helper (Th) 1/Th17 cells. Interferon-β (IFNβ) is widely used as a disease-modifying MS drug, but its effects on Th17 cells are still disputed. Furthermore, the effects of IFNβ on Th9 cells have not been elucidated. The present study aimed to clarify the effects of IFNβ on cytokines/growth factors in cerebrospinal fluid (CSF) and cytokine-producing Th cells in peripheral blood.

**Methods** First, the frequency of IFNγ, interleukin (IL)-17A, IL-9, and IL-4-producing Th cells in peripheral blood lymphocytes was analyzed by flow cytometry in 34 MS patients and 15 healthy volunteers enrolled in the cytokine-producing Th cell study. Second, levels of 27 cytokines/growth factors in the CSF were measured using a multiple fluorescence bead-based immunoassay in 34 MS patients enrolled in the cytokines/growth factors study.

**Results** We found a significantly higher frequency of IL-4−IL-9+CD4+ T cells and lower frequency of IFNγ+IL-17A−CD4+ cells in peripheral blood lymphocytes in the 10 MS patients who had received IFNβ than in the 24 MS patients who had not received IFNβ or the 15 healthy controls ($P < 0.05$). The seven MS patients who received IFNβ showed significantly lower IL-17A levels in CSF than did the 27 MS patients who had not received IFNβ ($P < 0.05$).

**Conclusions** The present results suggest the suppression of IL-17A production in the central nervous system and augmentation of Th9 cells in the peripheral blood by IFNβ in MS patients.

## Introduction

Multiple sclerosis (MS) is an inflammatory demyelinating disease of the central nervous system (CNS), and is generally considered to be mediated by myelin-autoreactive T cells.[1] MS was believed to be a T helper (Th) 1-mediated autoimmune disease based on Th1/Th2 balance, but since the discovery of Th17 in experimental autoimmune encephalomyelitis (EAE), an animal model of MS, MS is currently considered to be a Th1/Th17 disease from the aspect of Th cell balance.[1,2] In contrast, interleukin-9 (IL-9)-producing T cells, Th9 cells, are regarded as of a different lineage from Th1, Th2 and Th17 cells,[3] and myelin oligodendrocyte glycoprotein (MOG)-specific Th9 can induce experimental autoimmune encephalitis.[4] However, the role of Th9 cells in MS remains to be elucidated.

In a previous study, administration of interferon-γ (IFNγ) to MS patients exacerbated the MS, whereas interferon-β (IFNβ) suppressed the disease course.[5] Since then, IFNβ has become widely used as a disease-modifying drug in MS. Many studies suggest that IFNβ is multifunctional; that is, it has an

antiproliferative effect, blocks T cell activation, induces apoptosis of autoreactive T cells, antagonizes IFNγ, restores T regulatory cell activity, promotes the expression of neurotrophic factors, modulates cytokines, affects the blood–brain barrier (BBB) and shows antiviral effects.[6] Considering the effects of IFNβ on Th cells, we previously reported the inhibition of Th1 activation, induction of IL-4- and IL-13-producing Th2 cells, and Th2 shift by IFNβ in MS.[7] Although several studies have shows a suppressive or no effect of IFNβ on Th17/IL-17 in EAE and human MS, there have also been reports of no reduction of Th17 by IFNβ, but FTY720, as well as IFNβ resistance in MS patients who had higher IL-17F levels.[8–12] IFNβ added in Th9-polarizing culture conditions upregulated IL-9 production from T cells,[13] but the relationship between IFNβ therapy and Th9 in MS is unclear.

In the present study, we attempted to clarify the effects of IFNβ on *in vivo* cytokine production in MS. We examined Th cell profiles including IL-17A- and IL-9-producing Th cells in peripheral blood (PB) from MS patients receiving IFNβ, and explored the effects of IFNβ on cytokine/chemokine levels in cerebrospinal fluid (CSF).

## Methods

### Participants

All patients were examined at the Department of Neurology, Kyushu University Hospital, Japan. Informed consent was obtained from each individual, and the study protocol was approved by the ethics committee of the hospital. A total of 34 patients who were diagnosed with clinically definite MS based on Poser's criteria[14] and 15 healthy controls (HC) were enrolled in the PB Th cell study between December 2009 and February 2011. Their fresh peripheral venous blood was obtained in the remission phase and used promptly. In addition, 34 patients with clinically definite MS took part in the CSF cytokine/growth factor study between 2000 and 2008. Their donated CSF was cryopreserved at −70°C in our laboratory. All patients were negative for anti-aquaporin 4 antibodies, measured by immunofluorescence as described previously.[15,16] The patients' disability was scored using the Expanded Disability Status Scale of Kurtzke.[17] Acute transverse myelitis was defined according to Fukazawa et al.[18] Longitudinally extensive spinal cord lesions were defined as spinal cord lesions extending three or more vertebral segments on magnetic resonance imaging.[19]

The demographic features of the MS patients are summarized in Tables 1 and 2. Among the 34 MS patients enrolled in the PB Th study, IFNβ had been given to 10 of them (29.4%) for 4.3 ± 3.3 years (range 0.1–9.1 years, median 5.6 years; blood samples were withdrawn at least 11 months after the initiation of IFNβ in all but one patient, from whom blood was taken approximately 1 month after IFNβ was initiated) at the time of donating the blood sample. Among the 34 patients enrolled in the CSF cytokine/chemokine study, IFNβ had been given to seven of them (20.6%) for 3.0 ± 2.1 years (range 1.0–6.2 years, median 1.3 years) at the time of donating the CSF sample. In patients without IFNβ treatment, seven patients in the PB Th study and three patients in the CSF cytokine/chemokine study had a history of IFNβ therapy; however, all of them had completed the therapy over a year before the study commenced. No patients had a history of

**Table 1** Demographic features of the participants in the peripheral blood by T helper cell study

| | MS patients ($n$ = 34) | IFNβ (−) ($n$ = 24) | IFNβ (+) ($n$ = 10) | HC ($n$ = 15) |
|---|---|---|---|---|
| No. males/females | 5/29 | 3/21 | 2/8 | 6/9 |
| RRMS/SPMS | 29/5 | 19/5 | 10/0 | – |
| Age at examination (years) | 45.0 ± 14.7 | 48.1 ± 15.3 | 37.9 ± 10.9 | 39.6 ± 16.7 |
| Disease duration (years) | 13.9 ± 11.5 | 15.7 ± 12.8 | 9.7 ± 6.2 | – |
| EDSS score at last visit | 3.38 ± 2.27 | 3.4 ± 2.2 | 3.5 ± 2.6 | – |
| Administration of prednisolone | 4/34 (11.8%) | 3/24 (12.5%) | 1/10 (10.0%) | – |
| Administration of immunosuppressants* | 3/34 (8.8%) | 3/24 (12.5%) | 0/10 (0.0%) | – |
| Administration of IFNβ1b/IFNβ1a | 7/3 | – | 7/3 | – |

EDSS, Expanded Disability Status Scale of Kurtzke; HC, healthy controls; IFNβ, interferon-β; MS, multiple sclerosis; RRMS, relapsing–remitting multiple sclerosis; SPMS, secondary progressive multiple sclerosis.

Mean ± SD is shown.

*Azathioprine 50 mg/day, azathioprine 100 mg/day or cyclosporine 150 mg/day.

**Table 2** Demographic features of multiple sclerosis patients in the cerebrospinal fluid cytokine/chemokine study

| | MS patients ($n$ = 34) | IFNβ (−) ($n$ = 27) | IFNβ (+) ($n$ = 7) |
|---|---|---|---|
| No. males/females | 11/23 | 9/18 | 2/5 |
| RRMS/SPMS | 32/2 | 26/1 | 6/1 |
| Relapse time (times) | 5.3 ± 4.3 | 5.0 ± 4.0 | 6.3 ± 5.8 |
| Age at onset (years) | 31.6 ± 10.1 | 32.1 ± 10.0 | 30.0 ± 11.2 |
| Disease duration (years) | 6.9 ± 7.1 | 6.7 ± 7.2 | 7.9 ± 7.3 |
| EDSS score at last visit | 3.4 ± 2.4 | 3.1 ± 2.4 | 4.6 ± 2.5 |
| Severe visual impairment (≥FS 5) | 7/34 (20.6%) | 6/27 (22.2%) | 1/7 (14.3%) |
| Acute transverse myelopathy | 6/34 (17.6%) | 4/27 (14.8%) | 2/7 (28.6%) |
| LESCL during entire course | 11/34 (32.4%) | 9/27 (33.3%) | 2/7 (28.6%) |
| Administration of prednisolone | 12/34 (35.3%) | 7/27 (25.9%) | 5/7 (71.4%) |
| Dose of prednisolone (mg) | 6.2 ± 13.1 | 6.0 ± 15.3 | 8.6 ± 10.7 |
| Cell counts of CSF (/μL) | 4.9 ± 7.3 | 5.5 ± 8.1 | 2.4 ± 1.3 |
| Protein levels of CSF (mg/dL) | 35.0 ± 18.0 | 36.8 ± 19.4 | 28.0 ± 9.6 |
| Remission/relapse phase | 15/19 | 13/14 | 2/5 |
| Administration of immunosuppressants | 0/34 (0.0%) | 0/27 (0.0%) | 0/7 (0.0%) |
| Administration of IFNβ1b/IFNβ1a | 6/1 | – | 6/1 |

CSF, cerebrospinal fluid; EDSS, Expanded Disability Status Scale of Kurtzke; IFNβ, interferon-β; LESCL, longitudinally extensive spinal cord lesion; RRMS, relapsing–remitting multiple sclerosis; SPMS, secondary progressive multiple sclerosis.
Mean ± SD is shown.

receiving disease-modifying therapies except IFNβ or intravenous immunoglobulin in either study. There were no significant differences in demographic features between patients who had and had not received IFNβ in either the PB Th or CSF cytokine/growth factor studies.

### Analysis of cytokine-producing Th cells in peripheral blood

Fresh peripheral venous blood was obtained from 34 MS patients and 15 HC. PB mononuclear cells were separated by Ficoll-Paque PLUS (GE Healthcare, Piscataway, NJ, USA) gradient centrifugation. All blood samples were taken during a remission phase. The following monoclonal antibodies were used: for flow cytometric analysis, anti-human CD4-APC (BD Biosciences, San Jose, CA, USA), anti-human IFN-γ-PE (BD Biosciences), anti-human IL4-FITC (Biolegend, San Diego, CA, USA), anti-human IL9-PE (Biolegend) and anti-human IL17AA-FITC (Biolegend); for intracellular staining, cells were stimulated for 4 h with phorbol 12-myristate 13-acetate (10 ng/mL) and ionomycin (1 μg/mL; both from Enzo Life Sciences, Plymouth Meeting, PA, USA) in the presence of Brefeldin A (Sigma Aldrich, St. Louis, MO, USA), fixed and permeabilized using BD FACS lysing solution and BD FACS permeabilizing solution (BD Biosciences) according to the manufacturer's instructions. Data were acquired on a MAQSQuan analyzer (Miltenyi Biotec, Bergisch Gladbach, Germany) and analyzed with MAQSQuantify software (Miltenyi Biotec). The frequencies of CD4+ cells expressing IFNγ, IL-17A, IL-9 or IL-4 in PB lymphocytes were measured.

### Analysis of cytokine/chemokine levels in CSF

CSF samples were taken from 19 patients within 1 month of the start of a relapse and before administration of intravenous methylprednisolone (14 patients who did not receive IFNβ and 5 who did receive IFNβ), and from 15 patients during the remission phase (13 patients who did not receive IFNβ and 2 who did receive IFNβ). The liquid phase of the CSF was simultaneously analyzed for 27 cytokines/chemokines and growth factors, namely: IL-1β, IL-2, IL-4, IL-5, IL-6, IL-7, IL-9, IL-10, IL-12/p70, IL-13, IL-15, IL-17A, IFNγ, tumor necrosis actor-α, IL-8/C-X-C motif ligand 8 (CXCL8), CXCL10/inducible protein 10 (IP-10), CCL2, CCL3/macrophage inflammatory protein (MIP)-1α, CCL4/MIP-1β, CCL5/RANTES, CCL11/eotaxin, granulocyte colony stimulating factor (CSF3), granulocyte-macrophage colony stimulating factor (CSF2), platelet-derived growth factor beta (PDGFβ), basic fibroblast growth factor (FGF2), vascular endothelial growth factor (VEGF) and IL-1 receptor antagonist (IL1RA). The Bio-Plex Cytokine Assay System (Bio-Rad Laboratories, Hercules, CA, USA) was used according to the manufacturer's instructions. The detailed methodology has been described in our previous report.[20]

### Statistical analysis

The significance of differences was assessed using the $\chi^2$-test, or Fisher's exact probability test when the criteria for the $\chi^2$-test were not fulfilled to compare categorical variables. For comparison of continuous values, we used the non-parametric Kruskal–Wallis $H$-test for non-normally distributed variables. When statistical significance was found, the Mann–Whitney $U$-test was then used to determine the statistical differences between groups.

Clinical & Experimental
Neuroimmunology

Clinical and Experimental Neuroimmunology **5 (Suppl. 1)**, (2014) 2–3

EDITORIAL

# Molecular targeted therapy in multiple sclerosis: Bench to bedside and bedside to bench

Multiple sclerosis (MS) is the prototypical inflammatory demyelinating disease of the central nervous system (CNS). It is indubitably an immune mediated disease, and is typified pathologically by multiple inflammatory foci, plaques of demyelination and neuroaxonal pathology that is considered to be associated with most of the long-term disability. However, its etiology remains a mystery, and its pathogenesis is only partly understood.

Animal models for human diseases are powerful tools, not only for studying disease pathogenesis, but also for drug discovery in terms of delineating specific targets related to disease mechanisms and developing effective molecules for clinical application. MS is a complex disease with heterogeneous clinical and pathological phenotypes that can vary from individual to individual. Hence, there is no single animal model that could encompass the full spectrum of clinical and pathological manifestations of MS. So far, experimental autoimmune encephalomyelitis (EAE) is the most commonly used animal model of MS, and there are currently several pathophysiological forms of EAE with varying patterns of clinical and pathological presentation depending on animal species, central nervous system (CNS) autoantigens and immunization protocols. Although there are differences between the pathophysiology of EAE and MS, an enormous amount of work has been carried out in finding pathogenetic immune pathways and immunomodulatory strategies both in EAE and in MS. As a result, EAE has provided a good opportunity to gain insights into the underlying immunopathogenesis of MS. Furthermore, many of the current and emerging disease-modifying drugs (DMD) and immunotherapeutic strategies with selective actions that target biological molecules involved in MS pathogenesis have been developed, validated and tested on the basis of EAE studies. In this special issue of *Clinical and Experimental Neuroimmunology*, immunological aspects of molecular targeted therapy in MS are described in four review articles.

EAE is considered to be most useful in evaluating the efficacy of certain targets for MS therapies, because this model is based on the concept that autoimmune responses against myelin antigens cause inflammatory demyelination in the CNS. Thus, many therapeutic targets for MS have been extensively screened for their efficacy in EAE. However, there are many examples of therapies that showed incredible promise in EAE, which have not translated into successful therapies in MS.[1] This is one of the criticisms of EAE. The reasons for translational failures are complicated, but such results provide the opportunity to rethink the pathogenesis of MS and lead to other therapeutic approaches. Some of these examples are antibodies directed to deplete T cells (anti-CD3 and anti-CD4 antibodies) and oral tolerogens.

There are also other therapeutic agents that have been proved to be of benefit both in EAE and in MS. Interferon-beta, glatiramer acetate, natalizumab (α4-integrin antagonist), and more recently fingolimod (functional antagonist against sphingosine-1-phosphate receptor) are good examples of convincing correlations between EAE and MS therapy. Interferon-beta and glatiramer acetate are widely used DMD for the first-line treatment of relapsing–remitting MS, but the mechanisms behind the therapeutic benefits of these drugs are incompletely elucidated. Therefore, investigating the mechanisms of their action can provide a deeper understanding of the molecular mechanisms involved in MS pathogenesis. α4-Integrin has been shown to be an essential molecule in EAE, and natalizumab, a monoclonal antibody against α4-integrin, is one of the most successful DMD that came from EAE studies. However, this drug was reported to be associated with progressive multifocal leukoencephalopathy (PML), an opportunistic infection due to the reactivation of John Cunningham virus. Because John Cunningham virus infects only humans, the development of PML was not predicted on the basis of EAE studies. The development of PML is thought to result from incomplete immune surveillance in the CNS, and natalizumab might show the potential risk of PML associated with drugs involved in blocking lymphocyte migration into the CNS.

There are a few examples of therapeutic agents that have shown remarkable success in MS without prior evaluation in EAE. Alemtuzumab, a monoclonal antibody against human CD52, was shown to be highly effective in suppressing the disease activity of relapsing–remitting MS.[2] Alemtuzumab does not cross-react with mouse CD52, and thus its effects in EAE had not been investigated until the transgenic mouse expressing human CD52 was developed. Daclizumab, a monoclonal antibody against the α-chain of the interleukin (IL)-2 receptor (CD25), showed a profound inhibition of inflammatory disease activity, and is currently being assessed in two phase III clinical trials for its efficacy in the treatment of patients with relapsing–remitting MS.[3] Although anti-CD25 monoclonal antibody is used to deplete or functionally inactivate CD4+CD25+Foxp3+ regulatory cells in mouse models of EAE, mechanistic studies of this therapy showed that daclizumab increased the number of immunoregulatory $CD56^{bright}$ NK cells, and this result provided a novel insight on the biology of IL-2 and IL-2 receptor interactions in the human immune system.[3] B-cell depletion therapy with rituximab, a monoclonal antibody against CD20, showed efficacy in reducing inflammatory brain lesions and clinical relapses in relapsing–remitting MS.[4] B-cell depletion therapy was not assessed in EAE before assessment in MS, because early studies in EAE suggested that B cells were dispensable for the induction of EAE. However, results from rituximab therapy in MS showed the absolutely essential role of B cells in MS pathogenesis, and a recent EAE study suggests that B-cell depletion is effective because B cells are major source of IL-6, which can help to drive Th17 antigen-specific responses.[5]

In conclusion, EAE has contributed to the development, validation and testing of novel MS drugs, and clinical trial results in MS also give us new and surprising information that we can then take back to the laboratory to understand the underlying mechanisms. In addition, the current MS drugs are entirely aimed at the relapsing stage of the disease, where inflammation is a predominant mechanism. In the progressive stage of the disease, neuroaxonal damage that is partially dissociated from inflammation became predominant. Because immunomoduratory and immunosuppressive treatments could have a marginal effect in the progressive stage, neuroprotective and reparative strategies need to be developed for this stage.

## Disclosure

Hirofumi Ochi is a consultant for Biogen Idec Japan.

## References

1. Wiendl H, Hohlfeld R. Therapeutic approaches in multiple sclerosis: lessons from failed and interrupted treatment trials. *BioDrugs*. 2002; **16**: 183–200.
2. Kousin-Ezewu O, Coles A. Alemtuzumab in multiple sclerosis: latest evidence and clinical prospects. *Ther Adv Chronic Dis*. 2013; **4**: 97–103.
3. Bielekova B. Daclizumab therapy for multiple sclerosis. *Neurotherapeutics*. 2013; **10**: 55–67.
4. Hauser SL, Waubant E, Arnold DL, et al. B-cell depletion with rituximab in relapsing-remitting multiple sclerosis. *N Engl J Med*. 2008; **358**: 676–88.
5. Barr TA, Shen P, Brown S, et al. B cell depletion therapy ameliorates autoimmune disease through ablation of IL-6-producing B cells. *J Exp Med*. 2012; **209**: 1001–10.

Hirofumi Ochi
*Department of Neurology, Ehime University Graduate School of Medicine, Toon, Ehime, Japan*

Genes and Immunity (2015) **16,** 54–56

**www.nature.com/gene**

**ORIGINAL ARTICLE**

# Associations of *HLA* class I alleles in Japanese patients with Crohn's disease

D Oryoji[1], T Hisamatsu[2], K Tsuchiya[3], J Umeno[4], S Ueda[1], K Yamamoto[5], T Matsumoto[4], M Watanabe[6], T Hibi[2,7] and T Sasazuki[1]

Previous studies have suggested that the human leukocyte antigen (HLA) is involved in the etiology of Crohn's disease (CD); however, few reports are available on the association between HLA class I antigens and CD in Japan. In this study, we performed association analysis of HLA class I antigens in CD using 208 Japanese patients and 384 healthy controls. We identified novel positive associations between CD and *HLA-A*02:01* (odds ratio (OR) = 1.64, $P = 0.016$) and *HLA-A*02:07* (OR = 2.31, $P = 0.0067$) and confirmed previously reported positive associations between CD and *HLA-Cw*14:02* (OR = 2.18, $P = 0.0021$) and *HLA-B*51:01* (OR = 1.70, $P = 0.033$). We also identified novel negative associations between CD and *HLA-A*24:02* (OR = 0.60, $P = 0.0047$) and *HLA-B*07:02* (OR = 0.38, $P = 0.0041$). Although the associations were not significant after full Bonferroni correction, we suggested that HLA class I genes have dual functions, susceptibility and resistance in controlling the development of CD.

*Genes and Immunity* (2015) **16,** 54–56; doi:10.1038/gene.2014.61; published online 6 November 2014

## INTRODUCTION

Crohn's disease (CD) and ulcerative colitis, two main subtypes of inflammatory bowel disease, are chronic and relapsing inflammatory disorders of the gastrointestinal tract caused by an aberrant response of the intestinal immune system to commensal bacteria.[1,2] CD affects all regions of the gastrointestinal tract, most commonly the ileum and colon, whereas the inflammation in ulcerative colitis is confined to the colon. The pathological changes in CD are typically discontinuous and often transmural. By contrast, those in ulcerative colitis are continuous and confined to the mucosa and submucosa.[2] Although the prevalence of CD is lower (23.6/100 000 persons) in Japan compared with European populations, it has been increasing continuously over the past several decades in Japan and other Asian countries.[3]

Although their exact etiology remains unclear, genetic factors appear to contribute to the susceptibility to these diseases. The genetic component seems stronger in CD than in ulcerative colitis.[4] A statistically significant association of human leukocyte antigen (HLA) with CD has been widely reported, especially for the *HLA* class II antigens;[5–9] reports of this association include a meta-analysis by Stokkers *et al.*[10] However, the data from these analyses should be interpreted with caution because they include data from both serological and molecular typing of *HLA*, as well as studies on different ethnic groups. There have been a few reports on the association of *HLA* class I alleles with CD in the Japanese population; however, there have been no reports specifically on the association of *HLA-A* alleles with CD in Japan. To elucidate the role of *HLA* class I antigens in the etiology of CD, we investigated the genetic association between the *HLA-A*, *-C* and *-B* alleles and CD in this study.

## RESULTS

### Association of HLA class I antigens with CD

We analyzed 10 *HLA-A*, 12 *HLA-C* and 18 *HLA-B* alleles with frequencies >1.0%. Compared with the controls, the antigen frequencies of *HLA-A*02:01* (odds ratio (OR) = 1.64, $P = 0.016$), *HLA-A*02:07* (OR = 2.31, $P = 0.0067$), *HLA-Cw*14:02* (OR = 2.18, $P = 0.0021$), *HLA-B*46:01* (OR = 1.88, $P = 0.018$) and *HLA-B*51:01* (OR = 1.70, $P = 0.033$) were increased in patients with CD, whereas the antigen frequencies of *HLA-A*24:02* (OR = 0.60, $P = 0.0047$) and *HLA-B*07:02* (OR = 0.38, $P = 0.0041$) were decreased (Table 1). Thus, we identified three novel susceptibility alleles for CD, *HLA-A*02:01*, *HLA-A*02:07* and *HLA-B*46:01*, and we confirmed two previously reported susceptibility alleles for CD, *HLA-Cw*14:02* and *HLA-B*51:01*.[11] Furthermore, we identified two novel protective alleles for CD, *HLA-A*24:02* and *HLA-B*07:02*. However, it should be noted that these associations were not statistically significant after Bonferroni correction. Therefore, the associations newly found in our study need to be replicated using another sample set in future study.

Among the three novel susceptibility alleles, linkage disequilibrium (LD) is known to occur between *HLA-A*02:07* and *HLA-B*46:01* in the Japanese population. Conditional analyses showed that *HLA-A*02:07* affected the strength of the association between *HLA-B*46:01* and CD and vice versa (Table 2). This observation, along with the fact that the association for *HLA-A*02:07* was more significant than the association for *HLA-B*46:01* in the non-conditional analysis (Table 1), suggests that *HLA-A*02:07* is the primary susceptibility allele for CD.

The novel protective alleles, *HLA-A*24:02* and *HLA-B*07:02*, are also known to be in LD in the Japanese population. However, we observed that the associations between these alleles and CD were still significant even when conditioned on each other (Table 2).

[1]Institute for Advanced Study, Kyushu University, Fukuoka, Japan; [2]Division of Gastroenterology and Hepatology, Department of Internal Medicine, School of Medicine, Keio University, Shinjuku-ku, Tokyo, Japan; [3]Department of Advanced Therapeutics for Gastrointestinal Diseases, Graduate School, Tokyo Medical and Dental University, Bunkyo-ku, Tokyo, Japan; [4]Department of Medicine and Clinical Science, Graduate School of Medical Sciences, Kyushu University, Fukuoka, Japan; [5]Department of Medical Chemistry, Kurume University School of Medicine, Fukuoka, Japan; [6]Department of Gastroenterology and Hepatology, Graduate School, Tokyo Medical and Dental University, Bunkyo-ku, Tokyo, Japan and [7]Center for Advanced IBD Research and Treatment, Kitasato University Kitasato Institute Hospital, Minato-ku, Tokyo, Japan. Correspondence: Professor T Sasazuki, Institute for Advanced Study, Kyushu University, 3-1-1 Maidashi, Higashi-ku, Fukuoka 812-8582, Japan.
E-mail: sasazuki@bioreg.kyushu-u.ac.jp
Received 31 May 2014; revised 29 August 2014; accepted 12 September 2014; published online 6 November 2014

This observation suggests that *HLA-A*24:02* and *HLA-B*07:02* are independent protective HLA class I alleles for CD. In conclusion, we identified *HLA-A*02:01* and *HLA-A*02:07* as novel *HLA* class I susceptibility alleles for CD and *HLA-A*24:02* and *HLA-B*07:02* as HLA class I protective alleles for CD.

LD structure between *HLA-A*24:02, HLA-Cw*14:02* and *HLA-B*51:01*

Although we found the *HLA-A*24:02* allele to be protective and the *HLA-Cw*14:02* and *HLA-B*51:01* alleles to be associated with susceptibility for CD, these alleles constitute a common HLA haplotype in the Japanese population. Therefore, we investigated the differences in the degree of LD among these alleles between the CD and control groups. As shown in Figure 1, moderate or strong LDs were observed between *HLA-A*24:02* and *HLA-Cw*14:02* ($D' = 0.36$), between *HLA-A*24:02* and *HLA-B*51:01* ($D' = 0.51$) and between *HLA-Cw*14:02* and *HLA-B*51:01* ($D' = 0.97$) in the control group. In contrast, although the LD between *HLA-Cw*14:02* and *HLA-B*51:01* was at the same level ($D' = 0.97$) in the CD group, the LDs between *HLA-A*24:02* and *HLA-Cw*14:02* and those between *HLA-A*24:02* and *HLA-B*51:01* were weaker in the CD group ($D' = 0.13$ and 0.06, respectively) than in the controls. These results suggest that the *HLA-A*24:02-Cw*14:02-B*51:01* haplotype carries unobserved variant adjacent to *HLA-A*24:02*, which contributes to a protective effect on CD.

**Table 1.** Association of *HLA* class I with CD

| *HLA allele* | *Antigen frequency (count)* | | P-*value* | *OR (95% CI)* |
|---|---|---|---|---|
| | *CD* (n = *208*) | *Controls* (n = *384*) | | |
| *HLA-A* | | | | |
| *A*02*[a] | 0.50 (105) | 0.36 (123) | $3.8 \times 10^{-4}$ | 1.92 (1.34–2.76) |
| *A*02:01* | 0.29 (60) | 0.20 (76) | 0.016 | 1.64 (1.10–2.44) |
| *A*02:07* | 0.12 (25) | 0.060 (23) | 0.0067 | 2.31 (1.26–4.24) |
| *A*24:02* | 0.50 (104) | 0.62 (239) | 0.0047 | 0.60 (0.43–0.86) |
| *HLA-C* | | | | |
| *Cw*14:02* | 0.19 (39) | 0.099 (38) | 0.0021 | 2.18 (1.33–3.57) |
| *HLA-B* | | | | |
| *B*07:02* | 0.058 (12) | 0.14 (53) | 0.0041 | 0.38 (0.20–0.73) |
| *B*46:01* | 0.15 (32) | 0.094 (36) | 0.018 | 1.88 (1.11–3.16) |
| *B*51:01* | 0.20 (41) | 0.13 (49) | 0.033 | 1.70 (1.07–2.70) |

Abbreviations: CA, Crohn's disease, OR, odds ratio CI, confidence interval.
[a]HLA-A*02:01, HLA-A*02:06 and HLA-A*02:07 were combined.

## DISCUSSION

In our study, novel positive associations between the *HLA-A*02:01* and *HLA*-A*02:07 alleles and CD were identified. Likewise, a serologically defined *HLA-A2* allele has been previously identified as a significant susceptibility allele for CD in Caucasians.[12] Therefore, we analyzed the total frequency of all *HLA-A*02* subtypes that were increased in CD, which included *HLA-A*02:01*, *HLA-A*02:06* and *HLA-A*02:07* (OR = 1.92, $P = 3.8 \times 10^{-4}$) (Table 1).

Among the *HLA-A*02* alleles, *HLA-A*02:07* was more strongly associated with CD than was *HLA-A*02:01*, and *HLA-A*02:06* did not exhibit a significant positive association. To explain these differences, we compared the amino acid sequences of each *HLA-A*02* allele subtype. There is a polymorphic change from phenylalanine to tyrosine at amino acid position 9 in the *HLA-A*02:06* allele compared with the susceptibility alleles *HLA-A*02:01* and *HLA-A*02:07*, which is not associated with CD susceptibility,

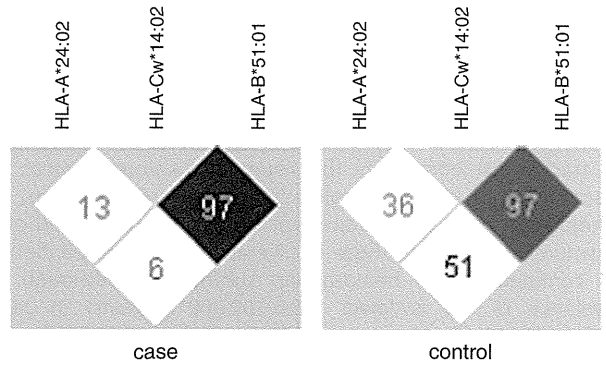


**Figure 1.** LD between the protective *HLA-A*24:02* allele and the susceptible *HLA-Cw*14:02* and *HLA-B*51:01* alleles for CD in cases and controls. The D′ values are indicated in each box.

**Table 2.** Conditional analyses of the associations between *HLA* class I and CD.

| *HLA* | *Non-conditioned* | *Conditioned with* | |
|---|---|---|---|
| | | *A*02:07* | *B*46:01* |
| *Susceptibility allele* | | | |
| *A*02:01* | 0.016 (1.64, 1.10–2.44) | NA | 0.012 (1.67, 1.11–2.50) |
| *A*02:07* | 0.0067 (2.31, 1.26–4.24) | NA | 0.12 (1.87, 0.85–4.11 |
| *Cw*14:02* | 0.0021 (2.18, 1.33–3.57) | 0.0011 (2.29, 1.39–3.78) | 0.0013 (2.26, 1.37–3.72) |
| *B*46:01* | 0.018 (1.88, 1.11–3.16) | 0.41 (1.33, 0.68–2.63 | NA |
| *B*51:01* | 0.033 (1.70, 1.07–2.70) | 0.018 (1.76, 1.10–2.82) | NA |
| | | *A*24:02* | *B*07:02* |
| *Protective allele* | | | |
| *A*24:02* | 0.0047 (0.60, 0.43–0.86) | NA | 0.017 (0.65, 0.46–0.93) |
| *B*07:02* | 0.0041 (0.38, 0.20–0.73) | 0.012 (0.42, 0.22–0.83) | NA |

The *P*-values (OR, 95% confidence interval) obtained by conditional logistic analysis using HLA-*A*02:07* or *HLA-B*46:01* as the susceptible *HLA* allele and using *HLA-A*24:02* or *HLA-B*07:02* as protective *HLA* alleles in a dominant model are indicated.

**Table 3.** Polymorphic amino acid changes among *HLA-A*02* alleles.

| *HLA-A*02* | *Polymorphic residue positions* | | | | |
|---|---|---|---|---|---|
| | *9* | *99* | *149* | *152* | *156* |
| *A*02:01* | F | Y | A | V | L |
| *A*02:06* | **Y** | Y | A | V | L |
| *A*02:07* | F | **C** | A | V | L |

The residues that are different among the three alleles are shown in bold face.

and a change from cysteine to tyrosine at position 99 in *HLA-A*02:01* compared with *HLA-A*02:07* (Table 3).[13]

It has been reported that the amino acids at positions 9 and 99 in HLA-A2 comprise the contact residues of the peptide binding pocket B. In these amino acid changes, the increased hydrophobicity of the residues at positions 9 and 99 has a greater effect on the susceptibility to CD (hydropathy index: phenylalanine 2.8, tyrosine −1.3, cysteine 2.5). The analysis of the amino acid changes among the *HLA-A*02:01*, *HLA-A*02:06* and *HLA-A*02:07* alleles suggests the following: (i) The phenylalanine at position 9 in *HLA-A*02* is critical to determine the susceptibility to CD. (ii) The change from cysteine to tyrosine at position 99 weakens the susceptibility to CD. In addition, *HLA-A*02:01* and *HLA-A*02:07* have been reported to bind peptides with leucine/methionine and leucine residues, respectively, at position 2, which is buried deep within peptide binding pocket B,[14,15] whereas *HLA-A*02:06* accommodates binding to valine/glutamine residues at position 2. These differences may also affect disease susceptibility to CD.

In summary, we identified two novel susceptibility HLA class I alleles, *HLA-A*02:01* and *HLA-A*02:07*, and two protective alleles, *HLA-A*24:02* and *HLA-B*07:02*, for CD in the Japanese population, although the association signals were not significant after full Bonferroni correction. It was suggested that the susceptibility conferred by the *HLA-A*02* alleles might be due to the polymorphic amino acid changes in these alleles that occur within pocket B in the antigen binding groove of the HLA-A2 molecule. All these findings may suggest a direct involvement of the HLA class I molecule in the susceptibility and resistance to CD by regulating the immune response in the gastrointestinal region.

## MATERIALS AND METHODS

### Subjects

Unrelated Japanese individuals with CD and healthy controls (208 and 384 individuals, respectively) were enrolled in this study. The CD diagnoses were made by gastroenterologists using conventional endoscopic, histologic and clinical criteria. Patients with indeterminate colitis were excluded in advance. Documented informed consent was obtained from each participant according to the Declaration of Helsinki. This study was also approved by the Ethics Committee at Kyushu University, Keio University and Tokyo Medical and Dental University in Japan.

### Genotyping of HLA alleles

We determined the *HLA-A*, *HLA-C* and *HLA-B* genotypes (4-digit) using the Luminex assay system (Luminex Corporation, Austin, TX, USA) and HLA typing kits (Wakunaga, Hiroshima, Japan). We observed a total of 79 alleles (*HLA-A*: 21, *HLA-C*: 18 and *HLA-B*: 40 alleles). The *HLA* alleles with a frequency >0.01 (*HLA-A*: 10, *HLA-C*: 12 and *HLA-B*: 18 alleles) were subjected to further analyses.

### Statistical analysis

The association between CD and the *HLA* class I antigen was assessed by logistic regression analysis with an allele dominant model adjusted for sex. For the conditional analysis, the indicated *HLA* class I allele was included in the independent variable. The *P*-values and ORs were computed using PLINK version 1.07 software (http://pngu.mgh.harvard.edu/purcell/plink/).[16] The LD among the *HLA* alleles (*HLA-A*24:02, HLA-Cw*14:02* and *HLA-B*51:01*) was calculated using Haploview version 4.2 software (http://www.broadinstitute.org/scientific-community/science/programs/medical-and-population-genetics/haploview/haploview).[17]

## CONFLICT OF INTEREST

The authors declare no conflict of interest.

## ACKNOWLEDGEMENTS

We thank all of the participants for providing blood samples. This work was supported by a Health Labour Sciences Research Grant for Research on Rare and Intractable Diseases from The Ministry of Health, Labour and Welfare, and by a Grant-in-Aid for Scientific Research on Innovative Areas, MEXT KAKENHI Grant Number 22133009, in Japan.

## REFERENCES

1 Podolsky DK. Inflammatory bowel disease. *N Engl J Med* 2002; **347**: 417–429.
2 Cho JH. The genetics and immunopathogenesis of inflammatory bowel disease. *Nat Rev Immunol* 2008; **8**: 458–466.
3 Asakura K, Nishiwaki Y, Inoue N, Hibi T, Watanabe M, Takebayashi T. Prevalence of ulcerative colitis and Crohn's disease in Japan. *J Gastroenterol* 2009; **44**: 659–665.
4 Xavier RJ, Podolsky DK. Unravelling the pathogenesis of inflammatory bowel disease. *Nature* 2007; **448**: 427–434.
5 Yoshitake SS. HLA class II alleles in Japanese patients with inflammatory bowel disease. *Tissue Antigens* 1999; **53**: 350–358.
6 Trachtenberg EA, Yang H, Hayes E, Vinson M, Lin C, Targan SR *et al.* HLA class II haplotype associations with inflammatory bowel disease in Jewish (Ashkenazi) and non-Jewish caucasian populations. *Hum Immunol* 2000; **61**: 326–333.
7 Nakajima AA, Matsuhashi N, Kodama T, Yazaki Y, Takazoe M, Kimura A. HLA-linked susceptibility and resistance genes in Crohn's disease. *Gastroenterology* 1995; **109**: 1462–1467.
8 Kawasaki A, Tsuchiya N, Hagiwara K, Takazoe M, Tokunaga K. Independent contribution of HLA-DRB1 and TNFα promoter polymorphisms to the susceptibility to Crohn's disease. *Genes Immun* 2000; **1**: 351–357.
9 Danzé P-M, Colombel JF, Jacquot S, Loste MN, Heresbach D, Ategbo S *et al.* Association of HLA class II genes with susceptibility to Crohn's disease. *Gut* 1996; **39**: 69–72.
10 Stokkers PC, Reitsma PH, Tytgat GN, van Deventer SJ. HLA-DR and -DQ phenotypes in inflammatory bowel disease: a meta-analysis. *Gut* 1999; **45**: 395–401.
11 Okada Y, Yamazaki K, Umeno J, Takahashi A, Kumasaka N, Ashikawa K *et al.* HLA-Cw*1202-B*5201-DRB1*1502 haplotype increases risk for ulcerative colitis but reduces risk for Crohn's disease. *Gastroenterology* 2011; **141**: 864–871.
12 Biemond I, Burnham WR, D'Amaro J, Langman MJ. HLA-A and -B antigens in inflammatory bowel disease. *Gut* 1986; **27**: 934–941.
13 Chen KY, Liu J, Ren EC. Structural and functional distinctiveness of HLA-A2 allelic variants. *Immunol Res* 2012; **53**: 182–190.
14 Falk K, Rotzschke O, Stevanovic S, Jung G, Rammensee HG. Allele-specific motifs revealed by sequencing of self-peptides eluted from MHC molecules. *Nature* 1991; **351**: 290–296.
15 Sudo T, Kamikawaji N, Kimura A, Date Y, Savoie CJ, Nakashima H *et al.* Differences in MHC class I self peptide repertoires among HLA-A2 subtypes. *J Immunol* 1995; **155**: 4749–4756.
16 Purcell S, Neale B, Todd-Brown K, Thomas L, Ferreira MA, Bender D *et al.* PLINK: a tool set for whole-genome association and population-based linkage analyses. *Am J Hum Genet* 2007; **81**: 559–575.
17 Barrett JC, Fry B, Maller J, Daly MJ. Haploview: analysis and visualization of LD and haplotype maps. *Bioinformatics* 2005; **21**: 263–265.

Journal of Alzheimer's Disease 44 (2015) 409–423
DOI 10.3233/JAD-141572
IOS Press



# Temporal Changes of CD68 and α7 Nicotinic Acetylcholine Receptor Expression in Microglia in Alzheimer's Disease-Like Mouse Models

Akihiro Matsumura[a], Syuuichirou Suzuki[a], Naotoshi Iwahara[a], Shin Hisahara[a], Jun Kawamata[a], Hiromi Suzuki[a], Ayano Yamauchi[a], Kazuyuki Takata[b], Yoshihisa Kitamura[b] and Shun Shimohama[a,*]
[a]*Department of Neurology, School of Medicine, Sapporo Medical University, Sapporo, Japan*
[b]*Department of Clinical and Translational Physiology, Kyoto Pharmaceutical University, Kyoto, Japan*

Accepted 2 September 2014

**Abstract**. We previously reported that activated microglia are involved in amyloid-β (Aβ) clearance and that stimulation of α7 nicotinic acetylcholine receptors (nAChR) in microglia enhances Aβ clearance. Nevertheless, how microglia and α7 nAChR in microglia are affected in Alzheimer's disease (AD) remains unknown. The present study aimed to collect fundamental data for considering whether microglia are potential targets for AD treatment and the appropriate timing of therapeutic intervention, by evaluating the temporal changes of Aβ, microglia, neurons, presynapses, and α7 nAChR by immunohistochemical studies in mouse models of AD. In an Aβ-injected AD mouse model, we observed early accumulation of CD68-positive microglia at Aβ deposition sites and gradual reduction of Aβ. Microglia were closely associated with Aβ deposits, and were confirmed to participate in clearing Aβ. In a transgenic mouse model of AD, we observed an increase in Aβ deposition from 6 months of age, followed by a gradual increase in microglial accumulation at Aβ deposit sites. Activated microglia in APdE9 mice showed two-step transition: a CD68-negative activated form at 6–9 months and a CD68-positive form from 12 months of age. In addition, α7 nAChR in microglia increased markedly at 6 months of age when activated microglia appeared for the first time, and decreased gradually coinciding with the increase of Aβ deposition. These findings suggest that early microglial activation is associated with α7 nAChR upregulation in microglia in APdE9 mice. These novel findings are important for the development of new therapeutic strategy for AD.

Keywords: α7 nAChR, Alzheimer's disease, amyloid-β, CD68, hippocampus, injections, microglia, phagocytosis, temporal, transgenic

## INTRODUCTION

Alzheimer's disease (AD) is characterized by extracellular senile plaques consisting of fibrillar amyloid-β (Aβ) peptides followed by the formation of neurofibrillary tangles and loss of synapses and neurons. Furthermore, deposition of Aβ is considered to be the most essential pathophysiological hallmark of AD according to the amyloid cascade hypothesis [1]. Nevertheless, the etiology of sporadic AD remains unknown. On the other hand, accumulation of activated microglia and astrocytes in and around senile plaques has been demonstrated in autopsied brains from AD patients, and considered to represent immune responses in patients with AD [2–7].

Microglia are macrophage-like resident immune cells in the central nervous system (CNS). We previously showed that microglia phagocytosed Aβ in

*Correspondence to: Dr. Shun Shimohama, Department of Neurology, School of Medicine, Sapporo Medical University, South 1, West 16, Chuo-ku, Sapporo 060-8543, Japan. Tel.: +81 11 611 2111; Fax: +81 11 622 7668; E-mail: shimoha@sapmed.ac.jp.